EPJ Plus

EPJ.org
your physics journal

Eur. Phys. J. Plus (2017) **132**: 195 DOI 10.1140/epjp/i2017-11449-1

Lorentz force effect on mixed convection micropolar flow in a vertical conduit

Mohamed S. Abdel-wahed

Società Italiana di Fisica
Springer

Eur. Phys. J. Plus (2017) **132**: 195
DOI 10.1140/epjp/i2017-11449-1

THE EUROPEAN PHYSICAL JOURNAL PLUS

Regular Article

Lorentz force effect on mixed convection micropolar flow in a vertical conduit

Mohamed S. Abdel-wahed[a]

Basic Sciences Department, Faculty of Engineering at Benha, Benha University, Cairo, Egypt

Received: 21 January 2017 / Revised: 5 March 2017
Published online: 2 May 2017 –

Abstract. The present work provides a simulation of control and filtration process of hydromagnetic blood flow with Hall current under the effect of heat source or sink through a vertical conduit (pipe). This work meets other engineering applications, such as nuclear reactors cooled during emergency shutdown, geophysical transport in electrically conducting and heat exchangers at low velocity conditions. The problem is modeled by a system of partial differential equations taking the effect of viscous dissipation, and these equations are simplified and solved analytically as a series solution using the Differential Transformation Method (DTM). The velocities and temperature profiles of the flow are plotted and discussed. Moreover, the conduit wall shear stress and heat flux are deduced and explained.

1 Introduction

Micropolar fluids are fluids with a microstructure consisting of rigid, randomly oriented particles suspended in a viscous medium, such as polymeric fluids, animal blood, etc. The model of micropolar fluids introduced by Eringen [1] presents the theory of microfluids, which support stress moment, and body moments taking the influence of spin inertia into consideration. A subclass of these fluids is micropolar fluids, which exhibit microrotational effects and inertia. Many researchers have studied the applications of this class of fluids.

Seddeek [2] analyzed the effects of a magnetic field on the flow of a micropolar fluid past a continuously moving plate using the theory of micropolar fluids deduced by Eringen. Ishak *et al.* [3] investigated the effect of uniform or variable heat flux on the heat transfer over a stretching surface in micropolar fluids. Rahman *et al.* [4] presented a numerical analysis of the magnetohydrodynamic convective flow and heat transfer of a micropolar fluid past a continuously moving vertical porous plate under the effect of heat source and suction. Kim [5] studied the unsteady motion of the convection micropolar flow past a vertical plate in a porous medium. Abdel-Rahman *et al.* [6] studied the effect of heat generation and thermal radiation on an unsteady moving surface subjected to a micropolar fluid. Bhargava *et al.* [7] studied the mixed convection micropolar flow through a vertical circular pipe. Zueco *et al.* [8] extended the work of Bhargava by taking the motion of the micropolar fluid through a non-Darcian porous medium. Rashidi *et al.* [9] studied the problem of Zueco from the biomedical point of view, considering the MHD biorheological transport phenomena in a porous medium as a mathematical simulation of magnetic blood flow filtration. Beg *et al.* [10] resolved the problem of Rashidi using the differential transformation method without dealing with the physical side of the problem. Siddiqa *et al.* [11] suggested a periodic function for the magnetohydrodynamic natural convection flow of a micropolar fluid.

The movement of many small charge carriers (*i.e.* electrons, ions) through a conductor causes the Hall effect. When a magnetic field is present, these charges produce a force, called the Lorentz force. Without magnetic field, the charges follow straight paths between collisions with impurities. However, in the presence of a magnetic field their paths between collisions curve causing an accumulation on each side of the path. Nihan [12] studied the effect of the Hall current on the MHD fluid flow over a rotating disk with uniform radial electric field. Thamizhsudar *et al.* [13] studied the Hall current effects on a rotating MHD flow of an exponentially accelerated horizontal plate. Sheikholeslami *et al.* [14] investigated the magnetic field effects in the forced-convection flow of a nanofluid over a stretching surface. Sarma *et al.* [15] presented an analytic solution for unsteady MHD boundary layer under the effect of the Hall current, rotation and Soret effect over a moving vertical plate. Siddiqa *et al.* [16] studied the effect of the Hall current on

[a] e-mail: `eng_moh_sayed@live.com`

the MHD flow with strong cross-magnetic field. Abdel-wahed and collaborators [17,18] obtained a semi-analytical solution using the OHAM for MHD boundary layer over a rotating disk under the influence of Hall current with Joule heating. The term “Joule heating”, investigated by Abdel-wahed *et al.* [18], refers to the interaction between the moving particles that form the current and the molecules of the fluid.

The work of Rashidi *et al.* [9] presented the non-Newtonian characteristics of blood as a micropolar fluid, by taking the model of Eringen [1] and the filtration process as a porous medium using the Darcy-Forchheimer drag force model. This work aims at extending the model of Rashidi to simulate the filtration process of the hydromagnetic blood flow under the effect of Lorentz force and heat source/sink, taking the influence of viscous dissipation and Joule heating into the modelling. The model is simplified to a system of partial differential equations of one non-dimensional variable (η) and then solved analytically using DTM, which was discussed and applied by Rashidi *et al.* [19–21] and Beg *et al.* [22]. The obtained results were improved by using the Padé approximation technique, then examined with previous publications and they showed good agreement.

2 Formulation of the problem

The physical model (see fig. 1) of the problem considers the steady, laminar, incompressible mixed convection flow of an electrically conducting micropolar fluid with Hall current effect running upward through a vertical conduit. Let us assume that the conduit is subjected to a uniform perpendicular magnetic field of strength B_0. The effect of heat source or sink (Q) is applied due to the control of the flow (blood) temperature through the transportation process in bio-separation devices. Moreover, the medium is assumed to be porous and modeled as the non-Darcian drag force model of second-order resistance. The components of the flow velocities and microrotation are (u, v, w) and $(\omega_1, \omega_2, \omega_3)$ in the directions of increasing (r, θ, z), respectively. Since the motion is supposed to be rotationally symmetric and the conduit is long enough, these components lead to $u = u(r)$, $v = 0$, $w = w(r)$ and $\omega_1 = \omega_3 = 0$; $\omega_2 = \omega_2(r)$.

The system that describes the problem, according to the above assumptions, is [7,8]

$$\frac{\partial u}{\partial r} + \frac{u}{r} = 0 \tag{1}$$

$$\rho u \frac{\partial u}{\partial r} + \frac{\partial p}{\partial r} = (\mu + k^*)\left(\frac{\partial^2 u}{\partial r^2} + \frac{1}{r}\frac{\partial u}{\partial r} + \frac{u}{r^2}\right) - \frac{\sigma {B_0}^2}{(1+m^2)}u - \left(\frac{\mu}{K}\right)u - \left(\frac{b\rho}{K}\right)u^2 \tag{2}$$

$$\rho u \frac{\partial w}{\partial r} + \frac{\partial p}{\partial z} = (\mu + k^*)\left(\frac{\partial^2 w}{\partial r^2} + \frac{1}{r}\frac{\partial w}{\partial r}\right) + \frac{k^*}{r}\frac{\partial (r\omega)}{\partial r} + \rho F_z - \frac{\sigma {B_0}^2}{(1+m^2)}w - \left(\frac{\mu}{K}\right)w - \left(\frac{b\rho}{K}\right)w^2 \tag{3}$$

$$\rho u j \frac{\partial \omega}{\partial r} = \gamma\left(\frac{\partial^2 \omega}{\partial r^2} + \frac{1}{r}\frac{\partial \omega}{\partial r} - \frac{\omega}{r^2}\right) - k^*\left(2\omega + \frac{\partial w}{\partial r}\right) \tag{4}$$

$$\begin{aligned}\rho C_p u \frac{\partial T}{\partial r} &= k_f\left(\frac{\partial^2 T}{\partial r^2} + \frac{1}{r}\frac{\partial T}{\partial r}\right) + \sigma B_0^2\left(u^2 + w^2\right) + (\mu + k^*)\left[2\left(\frac{\partial u}{\partial r}\right)^2 + 2\left(\frac{u}{r}\right)^2 + \left(\frac{\partial w}{\partial r}\right)^2\right] \\ &\quad + 2k^*\left(\omega + \frac{1}{2}\frac{\partial w}{\partial r}\right)^2 - 2\beta_1\left(\frac{\omega}{r}\frac{\partial \omega}{\partial r}\right) + \gamma\left(\left(\frac{\partial \omega}{\partial r}\right)^2 + \frac{\omega^2}{r^2}\right) + Q,\end{aligned} \tag{5}$$

where (u, w) are the longitudinal velocities along the (r, z) directions, respectively, ω is the microrotation or angular velocity, ρ is the micropolar fluid density, μ is the viscosity, k^* is the vortex viscosity, p is pressure, F_z is the body force per unit mass in the longitudinal direction, σ is the electrical conductivity of the micropolar fluid, m is the Hall current parameter ($m = \tau_e \omega_e$, where τ_e is the electron collusion time and ω_e is cyclotron frequency), K is the permeability of the porous medium (hydraulic conductivity), b is the Forchheimer parameter (inertia coefficient), j is the Eringen microinertia per unit mass (microinertia density), γ is the spin gradient viscosity coefficient, C_p is the isobaric specific heat, k_f is the thermal conductivity coefficient, β_1 is the micropolar material coefficient.

We use the following boundary conditions:

$$\text{at} \quad r = 0; \quad \frac{\partial u}{\partial r} = \frac{\partial w}{\partial r} = 0, \quad \omega = 0, \quad \frac{\partial T}{\partial r} = 0, \tag{6}$$

$$\text{at} \quad r = a; \quad u = w = 0, \quad \frac{\partial u}{\partial r} = 0, \quad \omega = -\lambda\left(\frac{\partial w}{\partial r}\right), \quad T = T_w, \tag{7}$$

where a is the conduit radius, T_w is the conduit wall temperature, and λ is the boundary parameter (which lies in the range of 0 to 1). For $\lambda = 0$ (strong concentration of microelements), there is no slip condition and the closer

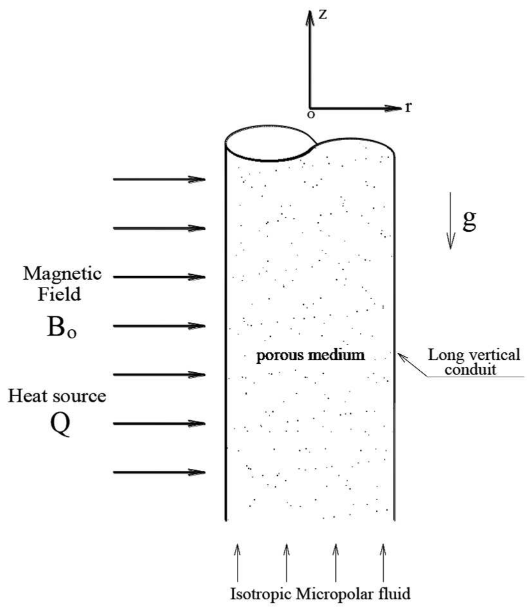

Fig. 1. Physical model and coordinate system.

microparticles to the conduit surface have no longitudinal velocity or rotation ($\omega = 0$). $\lambda \neq 0$ indicates that the effect of the microstructure near the conduit surface is negligible, since the suspended particles cannot get closer to the boundary than their radius. Due to the weak concentration of the microstructure, the value of this parameter is taken to be 0.5.

The body force term expressed as buoyancy term, such that $\rho F_z - \frac{\partial p}{\partial z} = 0$,

$$\rho F_z - \frac{\partial p}{\partial z} = (\rho - \rho_s)\, F_z - \frac{\partial (p - p_D)}{\partial z} \tag{8}$$

$$(\rho - \rho_s)\, F_z = -\beta \rho F_z\, (T - T_s) = -\beta \rho F_z \Theta, \tag{9}$$

where $\beta = \frac{(\rho - \rho_s)}{\rho (T_s - T)}$ is the volumetric expansion coefficient for small temperature difference and Θ is the dimensional temperature.

The boundary conditions (7) with eq. (1) give $u = 0$ and $\frac{\partial p}{\partial r} = 0$, so the pressure is a function of z only while w, ω, and Θ are functions of r only. Moreover, due to the long conduit, the pressure p can be taken equal to the hydrostatic pressure p_s, so $p_D = 0$.

Thus, the system (3)–(5) reduces to the following system of equations:

$$(\mu + k^*) \left(\frac{\partial^2 w}{\partial r^2} + \frac{1}{r} \frac{\partial w}{\partial r} \right) + \frac{k^*}{r} \frac{\partial (r\omega)}{\partial r} - \rho(\beta F_z \Theta) - \frac{\sigma {B_0}^2}{(1 + m^2)} w - \left(\frac{\mu}{K} \right) w - \left(\frac{b\rho}{K} \right) w^2 = 0 \tag{10}$$

$$\gamma \left(\frac{\partial^2 \omega}{\partial r^2} + \frac{1}{r} \frac{\partial \omega}{\partial r} - \frac{\omega}{r^2} \right) - k^* \left(2\omega + \frac{\partial w}{\partial r} \right) = 0 \tag{11}$$

$$k_f \left(\frac{\partial^2 \Theta}{\partial r^2} + \frac{1}{r} \frac{\partial \Theta}{\partial r} \right) + \sigma B_0^2 w^2 + (\mu + k^*) \left(\frac{\partial w}{\partial r} \right)^2 + 2k^* \left(\omega + \frac{1}{2} \frac{\partial w}{\partial r} \right)^2$$
$$- 2\beta_1 \left(\frac{\omega}{r} \frac{\partial \omega}{\partial r} \right) + \gamma \left(\left(\frac{\partial \omega}{\partial r} \right)^2 + \frac{\omega^2}{r^2} \right) + Q = 0. \tag{12}$$

We use the following dimensionless variables:

$$\eta = \frac{r}{a}\,, \qquad f(\eta) = \frac{a\rho}{\mu} w, \qquad g(\eta) = \frac{a^2 \rho}{\mu} \omega, \qquad \theta(\eta) = \frac{T - T_s}{T_w - T_s} = \frac{\Theta}{\Theta_w}\,, \qquad F = -F_z, \tag{13}$$

where η is the similarity variable. Substituting eq. (13) into eqs. (10)–(12), the following system of non-linear ordinary differential equations is obtained:

$$(1+E_r)\left[f''+\frac{1}{\eta}f'\right]+E_r\left[g'-\frac{1}{\eta}g\right]+G_r\theta-\frac{H_a^2\ell^2}{(1+m^2)}f-\frac{1}{D_a}f-\frac{F_s}{D_a}f^2=0 \tag{14}$$

$$A_1\left[g''+\frac{1}{\eta}g'-\frac{1}{\eta^2}g\right]-E_r\left(2g+f'\right)=0 \tag{15}$$

$$\theta''+\frac{1}{\eta}\theta'+\left(D_pH_a^2\ell^2\right)f^2+D_p\left(1+E_r\right)f'^2+2E_rD_p\left[g+\frac{1}{2}f'\right]^2-2D_pA_2\left[\frac{1}{\eta}gg'\right]+D_pA_1\left[\left(\frac{g}{\eta}\right)^2+g'^2\right]+\alpha=0. \tag{16}$$

The transformed boundary conditions are:

$$\text{at}\quad \eta=0;\quad f'(0)=0,\quad g(0)=0\quad\text{and}\quad \theta'(0)=0 \tag{17}$$

$$\text{at}\quad \eta=1;\quad f(1)=0,\quad g(1)=-\lambda f'(1)\quad\text{and}\quad \theta(1)=1, \tag{18}$$

such that $E_r=\frac{k^*}{\mu}$ is the Eringen parameter, $G_r=\frac{a^3\rho^2\beta F\Theta_w}{\mu^2}$ is the Grashof number, $H_a^2=\frac{{B_0}^2\sigma L^2}{\mu}$ is the Hartman number, $\ell=\frac{a}{L}$ is the geometric parameter, $D_a=\frac{K}{a^2}$ is the Darcy number, $F_s=\frac{b}{a}$ is the Forchgermer number, $D_p=\frac{\mu^3}{k_f a^2\rho^2\Theta_w}$ is the dissipation parameter, $A_1=\frac{\gamma}{\mu a^2}$, $A_2=\frac{\beta}{\mu a^2}$ are the material constants and $\alpha=\frac{a^2Q}{k_f\Theta_w}$ is the heat source parameter.

The physical quantities of interest are the conduit surface shear stress, τ_w, and the local Nusselt number, Nu, which are defined as

$$\tau_w=\frac{\mu^2(1+E_r)}{\rho a^2}\left[\frac{\mathrm{d}f}{\mathrm{d}\eta}\right]_{\eta=1},\qquad Nu=\left[\frac{\partial\theta}{\partial\eta}\right]_{\eta=1}. \tag{19}$$

3 Method of solution

Taking the one-dimensional differential transform [19–22] into each term of eqs. (14), (15) and (16), the following transforms are obtained:

$$\eta f\rightarrow\sum_{r=0}^{k}(F[k-r]\delta[r-1]),\qquad \eta^2f^2\rightarrow\sum_{r=0}^{k}(F[r]F[k-r]\delta[r-2]),\qquad f'\rightarrow(k+1)F[k+1]$$

$$\eta f''\rightarrow\sum_{r=0}^{k}(F[k-r+2](k-r+2)(k-r+1)\delta[r-1]),\qquad \eta^2f'\rightarrow\sum_{r=0}^{k}(F[k-r+1](k-r+1)\delta[r-2])$$

$$\eta^2f'^2\rightarrow\sum_{r=0}^{k}F[k-r+1]F[r+1](k-r+1)(r+1)\delta[r-2],\qquad g\rightarrow G[k],\qquad \eta g^2\rightarrow\sum_{r=0}^{k}G[r]G[k-r]\delta[r-1]$$

$$\eta^2gf'\rightarrow\sum_{r=0}^{k}(G[r]F[k-r+1](k-r+1)\delta[r-2]),\qquad \eta^2g\rightarrow\sum_{r=0}^{k}(G[k-r]\delta[r-2])$$

$$\eta g'\rightarrow\sum_{r=0}^{k}(G[k-r+1](k-r+1)\delta[r-1]),\qquad \eta\theta\rightarrow\sum_{r=0}^{k}\theta[k-r]\delta[r-1]$$

$$\eta g'^2\rightarrow\sum_{r=0}^{k}(G[k-r+1]G[r+1](k-r+1)(r+1)\delta[r-2]),\qquad \eta\theta'\rightarrow\sum_{r=0}^{k}(\theta[k-r+1](k-r+1)\delta[r-1])$$

$$\eta gg'\rightarrow\sum_{r=0}^{k}G[r]G[k-r+1](k-r+1)\delta[r-1],$$

$$\eta^2g''\rightarrow\sum_{r=0}^{k}(G[k-r+2](k-r+2)(k-r+1)\delta[r-2]),$$

$$\eta^2\theta''\rightarrow\sum_{r=0}^{k}(\theta[k-r+2](k-r+2)(k-r+1)\delta[r-2]),$$

where $F[k]$, $G[k]$ and $\theta[k]$ are the transformed functions of $f(\eta)$, $g(\eta)$ and $\theta(\eta)$, respectively, and are given by

$$f(\eta)=\sum_{k=0}^{\infty}F(k)\eta^k,\qquad g(\eta)=\sum_{k=0}^{\infty}G(k)\eta^k\quad\text{and}\quad\theta(\eta)=\sum_{k=0}^{\infty}\theta(k)\eta^k. \tag{20}$$

Substituting by the above transforms into eqs. (14), (15) and (16), one can obtain the following system of equations:

$$\begin{aligned}
&(1+E_r)\sum_{r=0}^{k}\left(F\left[k-r+2\right]\left(k-r+2\right)\left(k-r+1\right)\delta\left[r-1\right]\right)+\left(\left(1+E_r\right)\left(k+1\right)F\left[k+1\right]\right)-E_rG\left[k\right]\\
&+E_r\sum_{r=0}^{k}G[k-r+1](k-r+1)\delta[r-1]-\frac{1}{D_a}\sum_{r=0}^{k}(F[k-r]\delta[r-1])\\
&-\frac{F_s}{D_a}\sum_{r=0}^{k}(F[r]F[k-r]\delta[r-1])-\frac{\mathrm{Ha}^2\ell^2}{(1+m^2)}\sum_{r=0}^{k}(F[k-r]\delta[r-1])+\mathrm{Gr}\sum_{r=0}^{k}\left(\theta\left[k-r\right]\delta\left[r-1\right]\right)=0
\end{aligned}\tag{21}$$

$$\begin{aligned}
&A_1\sum_{r=0}^{k}\left(G\left[k-r+2\right]\left(k-r+2\right)\left(k-r+1\right)\delta\left[r-2\right]\right)+A_1\sum_{r=0}^{k}\left(G\left[k-r+1\right]\left(k-r+1\right)\delta\left[r-1\right]\right)-\left(A_1G[k]\right)\\
&-\left(E_r\sum_{r=0}^{k}\left(F\left[k-r+1\right]\left(k-r+1\right)\delta\left[r-2\right]\right)\right)-\left(2E_r\sum_{r=0}^{k}\left(G\left[k-r\right]\delta\left[r-2\right]\right)\right)=0
\end{aligned}\tag{22}$$

$$\begin{aligned}
&\sum_{r=0}^{k}\left(\theta\left[k-r+2\right]\left(k-r+2\right)\left(k-r+1\right)\delta\left[r-2\right]\right)+\sum_{r=0}^{k}\left(\theta\left[k-r+1\right]\left(k-r+1\right)\delta\left[r-1\right]\right)+\left(\alpha\delta\left(k-2\right)\right)\\
&+D_p\mathrm{Ha}^2\ell^2\sum_{r=0}^{k}F[r]F\left[k-r\right]\delta\left[r-2\right]+D_p\left(1+E_r\right)\sum_{r=0}^{k}F\left[k-r+1\right]F\left[r+1\right]\left(k-r+1\right)\left(r+1\right)\delta\left[r-2\right]\\
&+2D_pE_r\sum_{r=0}^{k}\left(G[r]G\left[k-r\right]\delta\left[r-2\right]\right)+2D_pE_r\sum_{r=0}^{k}\left(G[r]F\left[k-r+1\right]\left(k-r+1\right)\delta\left[r-2\right]\right)\\
&+0.5D_pE_r\sum_{r=0}^{k}\left(F\left[k-r+1\right]F\left[r+1\right]\left(k-r+1\right)\left(r+1\right)\delta\left[r-2\right]\right)\\
&-2D_pA_2\sum_{r=0}^{k}G[r]G\left[k-r+1\right]\left(k-r+1\right)\delta\left[r-1\right]+D_pA_1\sum_{r=0}^{k}G[r]G\left[k-r\right]\\
&+D_pA_1\sum_{r=0}^{k}G[k-r+1]G[r+1](k-r+1)(r+1)\delta[r-2]=0,
\end{aligned}\tag{23}$$

with the initial conditions

$$F(0)=a,\qquad F(1)=0,\qquad G(0)=1,\qquad G(1)=b,\qquad \theta(0)=c,\qquad \theta(1)=0. \tag{24}$$

The solution of the system (21)–(24) is obtained as a function of the unknown initial conditions, a, b and c, with the assistance of the Mathematica program. To get the values of these constants, the Padé approximation technique is applied with the governing conditions at $\eta\to 1$; $F=0$, $G=-0.5\,F'$ and $\theta=1$, using FindRoot built in function in the Mathematica program so that the required symbols can be obtained.

In order to check the accuracy of the method used, table 1 presents a comparison with the numerical solution used in Zueco *et al.* [8].

4 Results and discussion

This study focuses on the behavior of the MHD micropolar fluid flow (blood) through a vertical continuous conduit under the effect of Lorentz force and heat source or sink. The influence of the embedded parameters, such as Eringen parameter (E_r), Hartman number (H_a), Hall current parameter (m), dissipation parameter (D_p), and Darcy number (D_a), on the translation/microrotation velocities and the temperature profiles is shown in figs. 2–13.

Table 1. Velocity gradient and the temperature gradient at the conduit surface at $E_r = 3$, $A_1 = 0.5$, $D_a = F_s = 0.1$, $\mathrm{Gr} = 1$, $\lambda = 0.5$.

α	Ha	Present results		Zueco [8]	
		$f'(1)$	$\theta'(1)$	$f'(1)$	$\theta'(1)$
-1	0	0.1226	0.5000	0.1224	0.5000
	10	0.1194	0.5000	0.1193	0.5000
0	0	0.1380	0.0000	0.1379	0.0000
	10	0.1343	0.0000	0.1342	0.0000

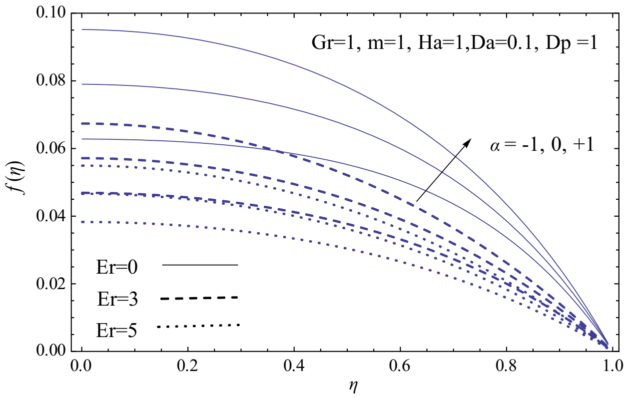

Fig. 2. Variation of the longitudinal velocity with the Eringen parameter.

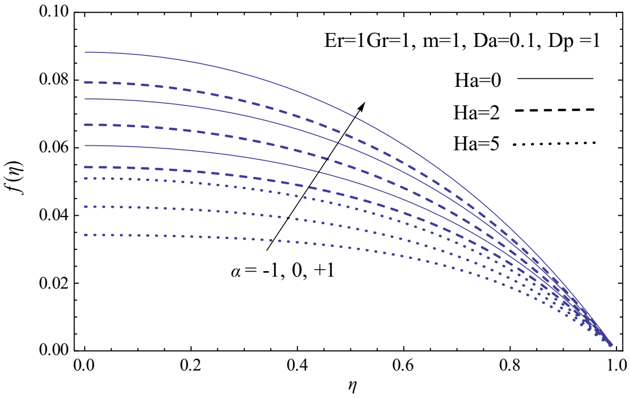

Fig. 3. Variation of the longitudinal velocity with the Hartman number.

The influence of all previous parameters is considered for the three cases of heat flow: $\alpha > 0$ corresponds to the heat source; $\alpha < 0$ corresponds to the heat sink; $\alpha = 0$ refers to no heat source effects. These cases may occur to control the flow temperature during the filtration process. Generally, figs. 2–7 show that the presence of a heat source increases the longitudinal and microrotation velocities due to the increase in the kinetic energy.

The Eringen parameter is the ratio between the vertex and kinematic viscosity. An increase in E_r induces a decrease in the longitudinal velocity, as is shown in fig. 2. It is clear that also for no vertex viscosity, $E_r = 0$ (Newtonian flow), the longitudinal velocity reaches its maximum at the center of the conduit. Moreover, presence of microelements within the flow increases the vertex viscosity, which triggers a decrease in the vertical flow.

The effect of the Hartman number (at constant Hall current effect) on the longitudinal velocity is presented in fig. 3, where the hydromagnetic term that contains the Hartman number describes a retarding force, which impedes flow in the normal direction to the applied magnetics strength. Therefore, a decrease in the transversal velocity occurs. It is worth mentioning that the Lorentz force vanishes at $H_a = 0$, which reduces the system to an electrically non-conducting micropolar fluid.

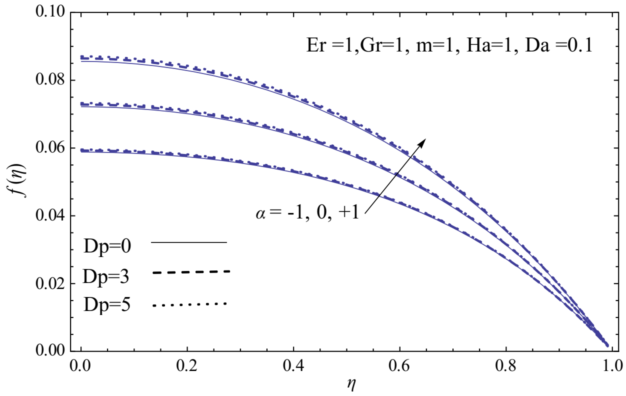

Fig. 4. Variation of the longitudinal velocity with the dissipation parameter.

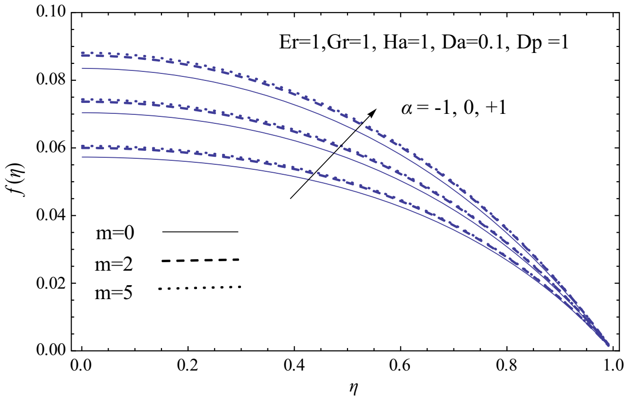

Fig. 5. Variation of the longitudinal velocity with the Hall current parameter.

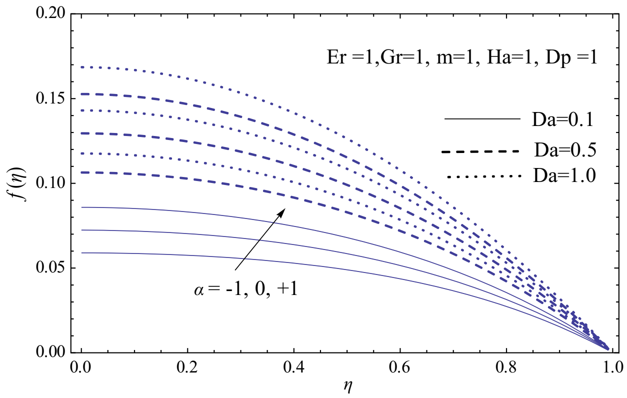

Fig. 6. Variation of the longitudinal velocity with the Darcy number.

The transformation of the kinetic energy due to the motion of the fluid to internal energy means heating up the fluid, which refers to viscous dissipation, the effect of the dissipation parameter D_p on the longitudinal velocity presented in fig. 4. We observe that the dissipation parameter has a limited effect on the velocity profiles in this direction. On the other hand, the movement of the small charge carriers through conductors causes the Hall effect, which raises the transversal velocity of the fluid particles, as shown in fig. 5.

Figure 6 shows the influence of the Darcy number on the transition. The Darcy number affects the permeability of the medium, such that for $D_a \to \infty$, the problem is reduced to hydromagnetic micropolar convection in pure fluid and an increase in D_a from 0.1, 0.5 to 1.0, indicating an increase of permeability, which induces an increase in the longitudinal velocity.

Figure 7 shows the variation of the rotational velocity under varying values of the Eringen parameter. Due to viscosity, which increases by increasing the Eringen parameter, the microrotational velocity decreases. This conclusion matches with the results obtained in [7].

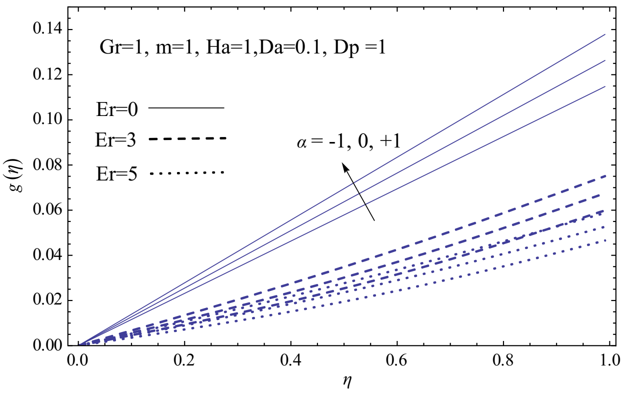

Fig. 7. Variation of the rotational velocity with the Eringen parameter.

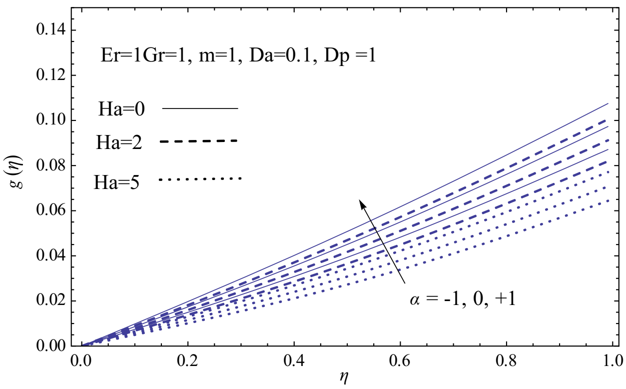

Fig. 8. Variation of the rotational velocity with the Hartman number.

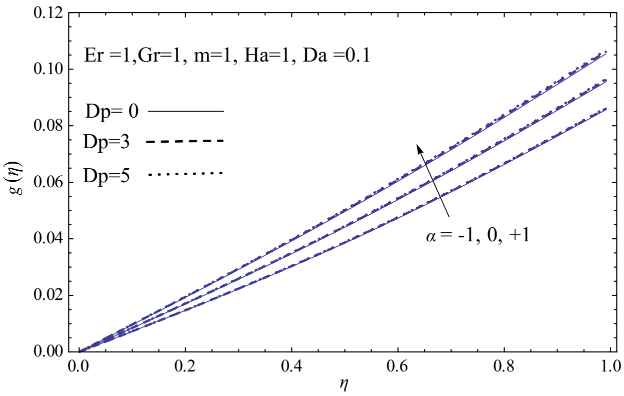

Fig. 9. Variation of the rotational velocity with the dissipation parameter.

Figure 8 depicts the variation of microrotation velocity under the effect of the Hartman number (at constant Hall current effect). Due to the increase in the magnetic strength, the microrotation velocity reduces although the term of magnetic force does not appear in the microrotaion equation (15); the microrotation is affected by the reduction in the longitudinal velocity. On the other hand, fig. 9 shows a limited increase in the rotational velocity under the increase in the viscous dissipation parameter.

Although the term that contains the Hall current parameter does not appear in the angular momentum equation, it has a perceptible effect on the microrotation velocity. Referring to fig. 10, one can observe that the Lorentz force results from the dual effect of the Hall current and the magnetic strength increases the microrotation velocity of the fluid. Referring to fig. 11, one can observe that due to an increase in the permeability of the medium, more space will be generated to increase the rotary velocity of the suspended microelements.

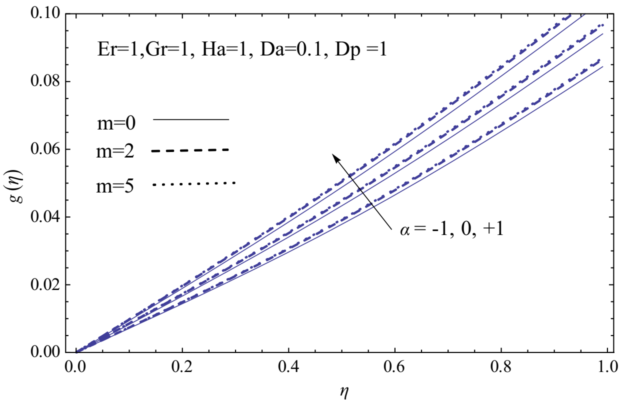

Fig. 10. Variation of the rotational velocity with the Hall current parameter.

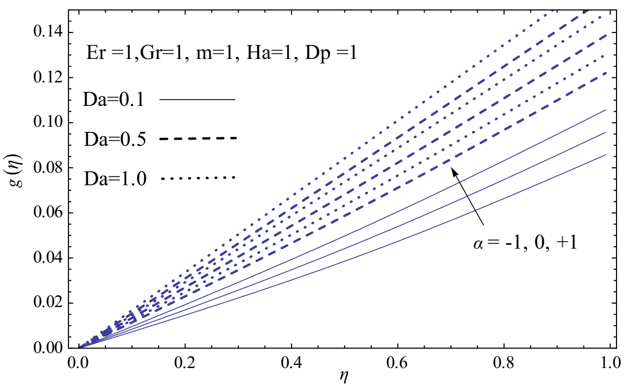

Fig. 11. Variation of the rotational velocity with the Darcy number.

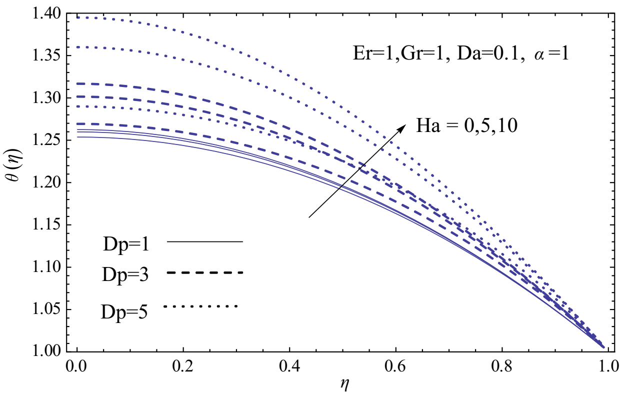

Fig. 12. Variation of the temperature with the dissipation parameter and the Hartman number.

The effect of the dissipation parameter D_p on the temperature profiles with the variation of the Hartman number is shown in fig. 12. It is clear that increasing the dissipation parameter as well as the Hartman number increases the internal energy of the fluid due to the increase in its kinetic energy, which makes the fluid temperature raise. Moreover, one can observe that the effect of magnetic strength (Hartman number) on the temperature is greater at high values of the dissipation parameter, such that increasing the Hartman number from zero to 5 makes the dimensionless temperature increase from 1.288 to 1.392, at $D_p = 5$, and from 1.255 to 1.263, at $D_p = 1$.

On the other hand, the effect of the dissipation parameter on the temperature profiles with the variation of the Eringen parameter is presented in fig. 13. Generally, one can observe that increasing the temperature will bring an increase in the Eringen parameter. However, the increase in the temperature depends on the value of the dissipation parameter D_p, such that, for $D_p = 1$, the Eringen parameter has a limited effect on the temperature profile compared to the profile at $D_p = 20$. It is worth mentioning that a high value of the dissipation parameter means that the fluid has a high range of internal energy.

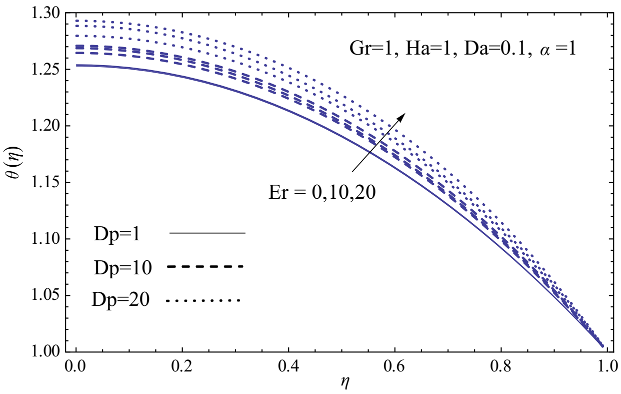

Fig. 13. Variation of the temperature with the dissipation parameter and the Eringen parameter.

Table 2. Velocity gradient and temperature gradient at $G_r = 1$, $\ell = 1$, $A_1 = 0.5$, $D_a = F_s = 0.1$, $D_p = \alpha = 1$.

E_r	m	Ha	$-f'(1)$	$-\theta'(1)$
0	0	0.0	−0.28343	−0.51274
		0.5	−0.28073	−0.51286
		1.0	−0.27305	−0.51315
	1	0.0	−0.28343	−0.51274
		0.5	−0.28209	−0.51304
		1.0	−0.27816	−0.51389
E_r	m	Ha	$-f'(1)$	$-\theta'(1)$
3	0	0.0	−0.15381	−0.52054
		0.5	−0.15271	−0.52037
		1.0	−0.14954	−0.51987
	1	0.0	−0.15381	−0.52054
		0.5	−0.15326	−0.52056
		1.0	−0.15166	−0.52061

Table 3. Velocity gradient and temperature gradient at $G_r = 3$, $\ell = 1$, $A_1 = A_2 = 0.5$, $D_a = F_s = 0.1$, $m = H_a = 1$, $\alpha = 1$.

E_r	D_p	$-f(1)$	$-\theta'(1)$
0	0.0	−0.27773	−0.50000
	1.0	−0.27816	−0.51389
	2.0	−0.27860	−0.52791
3	0.0	−0.15124	−0.50000
	1.0	−0.15166	−0.52061
	2.0	−0.15208	−0.54150

The influence of flow type (Newtonian/non-Newtonian), magnetic field with/without Hall current and viscous dissipation phenomena on the conduit surface shear stress and rate of heat transfer (Nusselt number) is presented in tables 2 and 3, where the Eringen parameter controls the type of flow, such that, at $E_r = 0$, the problem refers to a Newtonian flow and the other to a non-Newtonian flow. One can observe, from table 2, that the surface shear stress for the Newtonian flow is higher than that for the non-Newtonian flow and the opposite is true for the rate of heat transfer but by limited effect. In addition, table 2 shows a decrease in surface shear stress and an increase in the rate of heat transfer in the presence of a magnetic field. Moreover, the presence of the Hall current beside the magnetic field increases both shear stress and heat flux. On the other hand, table 3 presents the effect of the Eringen parameter with/without dissipation effects. It is clear that the presence of viscous dissipation increases the shear stress and heat flux and these increases are clearer for non-Newtonian flows.

5 Conclusion

- The longitudinal and microrotation velocities of the Newtonian flow through a vertical conduit are high with respect to those of the non-Newtonian flow in the presence of Hall effect, viscous dissipation and heat source/sink.
- Generally, the presence of heat source flow increases the microrotaion motion of the microparticles near the conduit surface.
- The influence of Hartman number and Eringen parameter on the flow temperature is greater active and clearer in the presence of strong viscous dissipation.
- The presence of Hall current in the MHD flow increases the surface shear stress and the rate of heat transfer.
- Viscous dissipation increases the surface shear stress and heat flux for a non-Newtonian flow more than for a Newtonian flow.

This study has no fund and the author declares that he has no conflict of interest.

References

1. A.C. Eringen, J. Appl. Math. Mech. **16**, 1 (1966).
2. M.A. Seddeek, Phys. Lett. A **306**, 255 (2003).
3. A. Ishak, R. Nazar, I. Pop, Phys. Lett. A **372**, 559 (2008).
4. M.M. Rahman, M.A. Sattar, J. Heat Transf. **128**, 142 (2005).
5. Y.J. Kim, Acta Mech. **148**, 105 (2001).
6. A.A. Saad, M.S. Abdel-wahed, Int. J. Energy Technol. **3**, 1 (2011).
7. R. Bhargava, R.S. Agarwal, L. Kumar, H.S. Takhar, Int. J. Eng. Sci. **42**, 13 (2004).
8. J. Zueco, O.A. Bég, H.S. Takhar, Comput. Mater. Sci. **46**, 1028 (2009).
9. M.M. Rashidi, M. Keimanesh, O.A. Bég, T.K. Hung, Int. J. Numer. Methods Biomed. Eng. **27**, 805 (2011).
10. T.A. Beg, M.M. Rashidi, O.A. Beg, N. Rahimzadeh, Comput. Methods Biomech. Biomed. Eng. **16**, 896 (2013).
11. S. Siddiqa, A. Faryad, N. Begum, M.A. Hossain, R.S. Gorla, Int. J. Thermal Sci. **111**, 215 (2017).
12. Nihan Uygun, J. Math. Stat. **44**, 1445 (2015).
13. M. Thamizhsudar, J. Pandurangan, R. Muthucumaraswamy, Int. J. Appl. Mech. Eng. **20**, 605 (2015).
14. M. Sheikholeslami, M.T. Mustafa, D.D. Ganji, Particuology **26**, 108 (2016).
15. D. Sarma, K.K. Pandit, Ain Shams Eng. J. (2016) DOI:10.1016/j.asej.2016.03.005.
16. S. Siddiqa, M.A. Hossain, R.S. Gorla, Int. J. Thermal Sci. **71**, 196 (2013).
17. M.S. Abdel-wahed, T.G. Emam, Thermal Sci. (2016) DOI: 10.2298/TSCI160312218A.
18. M.S. Abdel-wahed, M. Akl, AIP Adv. **6**, 095308 (2016).
19. M.M. Rashidi, S.A.M. Pour, N. Laraqi, Nonlinear Anal.: Model. Control **15**, 341 (2010).
20. M.M. Rashidi, E. Erfani, Comput. Fluids **40**, 172 (2011).
21. M.M. Rashidi, S.M. Sadri, Int. J. Comput. Methods Eng. Sci. Mech. **12**, 26 (2011).
22. T.A. Beg, M.M. Rashidib, O.A. Begc, N. Rahimzadeh, Comput. Methods Biomech. Biomed. Eng. **16**, 896 (2013).